Chemically induced folding of single and bilayer graphene†

Matthew J. Allen,[a] Minsheng Wang,[b] Sergio A. V. Jannuzzi,[a] Yang Yang,[c] Kang L. Wang[b] and Richard B. Kaner*[ac]

Received (in Cambridge, UK) 18th June 2009, Accepted 14th August 2009
First published as an Advance Article on the web 4th September 2009
DOI: 10.1039/b911972h

Here we report chemically induced folding of thin graphene flakes. The folding occurs spontaneously when an intercalating species interrupts the adhesion between graphene and a supporting substrate. The morphology of induced folds suggests that the conjugated π network is capable of extremely sharp curvature. Adjacent folds are often parallel, suggesting preferential deformation along certain crystallographic planes.

Since the initial experimental observation of single layers in 2004, graphene has been the focus of intense research.[1] High quality of the 2D crystal lattice results in many interesting properties, including exceptional carrier mobility and impressive mechanical strength.[2,3] This has motivated large efforts toward high-throughput syntheses, characterization techniques, and device fabrication.[4–8]

One of the most promising applications for graphene may be in the next generation of integrated circuits. In fact, carrier transport in graphene is approaching the ballistic region at low temperature.[9] So far, a major drawback of graphene-based field-effect transistors (FETs) has been their poor on/off ratios (usually just 10^3).[1] This is a direct consequence of a semi-metallic band structure in which the conduction and valence bands meet at a single Dirac point.[10,11] Resulting ambipolar conduction by either carrier type makes establishing an overall off state quite challenging. This problem has motivated a number of approaches toward band gap engineering in single layers, which would facilitate the fabrication of devices with more practical on/off ratios. Among these are functionalization of graphene's basal plane or its edges, substitutional doping of carbon with boron or phosphorus, and the use of quantum confinement in thin nanoribbons.[12–18] The initial goal of this work was the introduction of a band gap into bilayer graphene by varying interlayer distance and stacking by the intercalation of anions. The resulting broken symmetry has been proposed as one route toward the creation of a band gap.[19]

Anion intercalation of graphite upon exposure to oxidizing acids is well known. Typically done in the liquid phase, acid intercalation compounds can be prepared with interlayer spacing as large as 18.89 Å (for hydrated HF), as compared to 3.4 Å for native graphite.[20] For our experiments, graphene samples were prepared *via* mechanical exfoliation by cellophane tape on silicon substrates with thermally grown 300 nm oxide. The intercalation reaction was carried out at room temperature in the vapor phase by suspending the substrate just above the surface of a freshly prepared 3 : 1 volume ratio of H_2SO_4 : HNO_3. The vapor phase was used because submerging the substrate directly in the intercalating liquid results in complete delamination of the flakes. This mixture leads to the intercalation of negatively charged bisulfate ions (HSO_4^-) and an interlayer expansion to ~8 Å. After 1 minute of exposure to the vapors, the substrate was "rinsed" in streaming nitrogen to remove any condensed or residual acids from the surface.

Raman spectroscopy is a widely utilized tool in studies of graphene because the shape of the 2D band signal reflects direct changes in the electronic structure. This results in unique Raman signatures for single-, bi-, and multi-layer flakes, which can be used to quickly identify the number of layers present after mechanical exfoliation by cellophane tape or "peeling".[21–23] For characterizing graphite intercalation compounds (GICs), shifts and splitting of the G band signal indicate changes of the in-plane force constant. This provides a way to monitor the immediate chemical environment of individual sheets.

Fig. 1 shows the Raman spectra of a thick multi-layer flake, which we used to test our intercalation process, before and after vapor phase exposure to the acids. Before intercalation, pristine graphene shows a single peak G band corresponding to an in-plane vibrational mode (E_{2g2}) at 1582 cm^{-1}. After intercalation, it splits into two peaks, both blue shifted to 1585 cm^{-1} and 1600 cm^{-1}, respectively. Similar doublet structures have been observed in other studies of GICs and are attributed to the in-plane force constant difference between bounding and interior layers. Bounding layers are those directly adjacent to intercalant molecules and have larger modified force constants, which lead to a high-energy blue shift. Interior layers are not immediately adjacent to the intercalant, and its effects are screened somewhat.

After confirming the proficiency of vapor phase intercalation with a multi-layer flake, our attention shifted to thinner single- and bi-layers. In our original attempts to intercalate these thinner species, we were unable to find the flakes after exposure. Repeating the process in the presence of alignment markers enabled us to realize that the inability to locate and recognize flakes stemmed from significant changes in their shape and alignment upon intercalation. Similar changes were

[a] *Department of Chemistry and Biochemistry, University of California Los Angeles, LA, USA. E-mail: kaner@chem.ucla.edu; Tel: +1 310 825 5346*
[b] *Department of Electrical Engineering, University of California Los Angeles, LA, USA. E-mail: wang@ee.ucla.edu; Tel: +1 310 825 1609*
[c] *Department of Materials Science and Engineering, University of California Los Angeles, LA, USA. E-mail: yangy@ucla.edu; Tel: +1 310 825 4052*

† Electronic supplementary information (ESI) available: includes extended Raman spectra, optical images, and additional atomic force microscope data. See DOI: 10.1039/b911972h

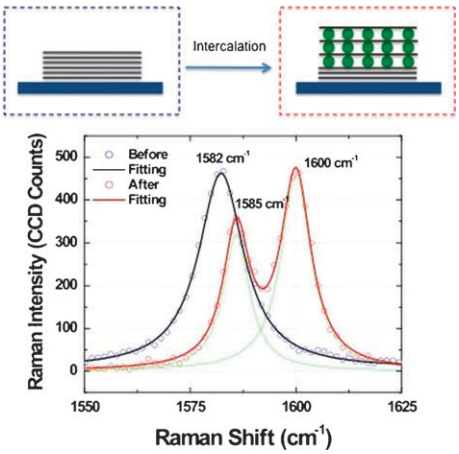

Fig. 1 A schematic diagram illustrates anion intercalation of thin graphene. G band Raman signal and fitting before (blue) and after (red) the intercalation process show that the in-plane vibrational mode at 1582 cm^{-1} splits upon intercalation into 2 peaks: 1585 cm^{-1} and 1600 cm^{-1}.

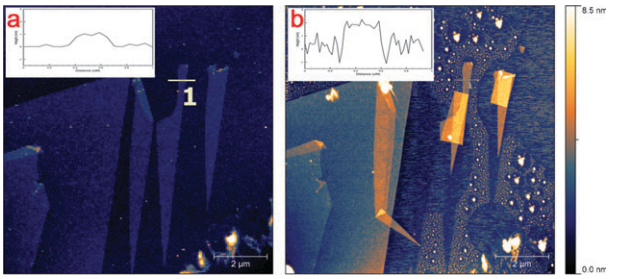

Fig. 3 Atomic force microscope images show three knife-shaped bilayers upon intercalation. Two of the flakes undergo nearly parallel folding, while the third relocates atop an adjacent bilayer. The inset line scans show a height profile expansion from (a) 0.7 nm to (b) ~2.0 nm.

demonstrated by another group recently with exposure to some organic solvents.[24]

Fig. 2 shows atomic force microscope (AFM) images taken before and after the intercalation of bilayer graphene flakes (as confirmed by step height analysis and Raman). As is evident in the images, the bilayers undergo a number of notable changes upon intercalation. First, an overall increase in thickness upon intercalation is highlighted by the colored scale bar. This was expected and is consistent with the incorporation of negatively charged bisulfate ions between the graphitic layers. Second, folding or crumpling is induced in many of the sheets upon exposure to the vapors. This is quite unexpected, as we previously conjectured that the adhesion force at the substrate–graphene interface would be sufficient to prevent motion or folding. Furthermore, the planar sp^2 network of graphene implies that folding should be a considerably high-energy process. We also note a shadow effect in the post-intercalation image created by a reaction between cellophane tape residue and the acidic vapors. The original flake positions have no tape residue, and hence remain unreacted and "clean" after exposure.

In order to better elucidate the effects of intercalation, a closer view of three knife-shaped bilayers is presented in Fig. 3. The inset line scans show an expansion of the height profile of an unmoved section of the middle flake from (a) 0.7 nm before intercalation to (b) ~2.0 nm after intercalation. Reacted adhesive is responsible for the large spikes in the post-intercalation line scan. The expected thickness of each sulfate ion is just over 0.5 nm, which suggests that the bilayer incorporates two layers of intercalant.[20] We believe that these two layers are comprised of one ion in between the graphitic layers and one ion in between graphene and the substrate. This conclusion is supported by the observation of complete delamination of some graphene flakes, including the left-most knife-shape in the figure (which relocated atop the adjacent mesa). Such delamination and relocation is likely only under a scenario in which the van der Waals forces between substrate and graphene are interrupted by an intercalant.

As in the case of the middle and right-most knife-shaped flakes in Fig. 3, some bilayers undergo folding instead of relocation once intercalation weakens the substrate adhesion force. We have made similar observations in the case of

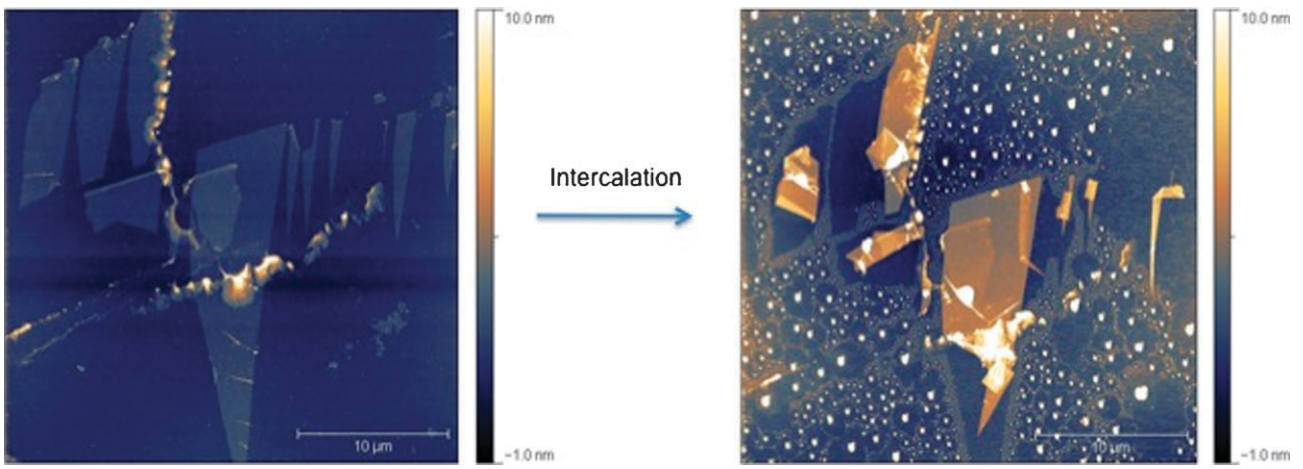

Fig. 2 Atomic force microscope images recorded before and after intercalation show changes in height profile along with folding and even delamination of some graphene flakes. A shadow effect in the post-intercalation image helps show the original flake positions and results from the reaction between cellophane tape residue and acid vapors.

single-layer graphene (See ESI†). As previously stated, the folding is unexpected due to the planarity of sp^2 bonding and the implied rigidity of graphene's honeycomb network. Several properties of the folds are noteworthy. First, multiple folds often occur in a parallel fashion, even for two spatially separated flakes. This may indicate preferential folding along one crystallographic or defect plane. This is consistent with the observation of "fault lines" made by Aksay *et al.* when manipulating single layers with scanning probe tips.[25] In addition, the atomic force microscope is unable to detect any rounding near the apparent creases, which instead appear as nearly 180° bends. One might infer that some oxidation takes place near the creases, changing the bonding hybridization to sp^3 and allowing the formation of a bend. The absence of any D band in the post-intercalation Raman spectrum indicates that essentially no such oxidation occurs (See ESI†). Instead, the sheets remain pristine and must undergo some induced strain.

The spontaneity of the folding suggests that it is a result of either (a) the intrinsic instability of planar single and bilayer graphene once unsupported by the substrate, or (b) some strong driving force that makes folding thermodynamically favorable. The stability of two-dimensional graphene (or lack thereof) has been the focus of much discussion as of late, with a number of groups commenting on the tendency for sheets to wrinkle or deform. In fact, Landau himself argued against the stability of two-dimensional crystals some 70 years ago.[26] In this case, however, the intercalant may well provide an additional driving force to encourage folding. The change in geometry upon folding leads to an increase in the total surface area of the carbon–carbon interfaces. This may allow the folded bilayer to incorporate more intercalant than possible in the planar case. Both conclusions suggest that mechanically exfoliated graphene may be more flexible than previously conjectured.

The ability shown here to induce folding provides access to graphene specimens with unique geometries. Although folded edges are often observed after mechanical exfoliation and have been induced previously through manipulation with a scanning probe tip, this is the first time that the phenomenon has been induced chemically. Scanning probe characterization of the flakes before and after folding may indeed show some interesting behavior near the creases and could potentially be used to quantify the forces necessary to induce folding. Electrical measurements may show whether carriers inside a folded flake flow in a continuous direction or if the high in-plane mobility leads them to follow the zigzag geometry of the individual sheets. In any event, it seems that intercalation of thin graphenes provides another way to probe the intrinsic qualities of this new and exciting material.

The authors thank the NSF IGERT program (MJA), FENA FCRP Center (MW, KLW and RBK), and the DARPA CERA program (KLW and RBK) for financial support. Instrumentation has been provided by the NanoPico Lab at the UCLA based California NanoSystems Institute.

Notes and references

1 K. S. Novoselov, A. K. Geim, S. V. Morozov, D. Jiang, Y. Zhang, S. V. Dubonos, I. V. Grigorieva and A. A. Firsov, *Science*, 2004, **306**, 666–669.
2 K. I. Bolotin, K. J. Sikes, Z. Jiang, M. Klima, G. Fudenberg, J. Hone, P. Kim and H. L. Stormer, *Solid State Commun.*, 2008, **146**, 351–355.
3 D. A. Dikin, S. Stankovich, E. J. Zimney, R. D. Piner, G. H. Dommett, G. Evmenenko, S. T. Nguyen and R. S. Ruoff, *Nature*, 2007, **448**, 457–460.
4 S. Stankovich, D. A. Dikin, G. H. B. Dommett, K. M. Kohlhaas, E. J. Zimney, E. A. Stach, R. D. Piner, S. T. Nguyen and R. S. Ruoff, *Nature*, 2006, **442**, 282–286.
5 K. S. Kim, *Nature*, 2009, **457**, 706–710.
6 V. C. Tung, M. J. Allen, Y. Yang and R. B. Kaner, *Nat. Nanotechnol.*, 2009, **4**, 25–29.
7 C. Berger, Z. M. Song, T. B. Li, X. B. Li, A. Y. Ogbazghi, R. Feng, Z. T. Dai, A. N. Marchenkov, E. H. Conrad, P. N. First and W. A. de Heer, *J. Phys. Chem. B*, 2004, **108**, 19912–19916.
8 W. A. de Heer, C. Berger, X. S. Wu, P. N. First, E. H. Conrad, X. B. Li, T. B. Li, M. Sprinkle, J. Hass, M. L. Sadowski, M. Potemski and G. Martinez, *Solid State Commun.*, 2007, **143**, 92–100.
9 X. Du, I. Skachko, A. Barker and E. Y. Andrei, *Nat. Nanotechnol.*, 2008, **3**, 491–495.
10 J. C. Slonczewski and P. R. Weiss, *Phys. Rev.*, 1958, **109**, 272–279.
11 P. R. Wallace, *Phys. Rev.*, 1947, **71**, 622.
12 H. Bai, Y. Xu, L. Zhao, C. Li and G. Shi, *Chem. Commun.*, 2009, 1667–1669.
13 D. W. Boukhvalov and M. I. Katsnelson, *Nano Lett.*, 2008, **8**, 4373–4379.
14 R. Hao, W. Qian, L. Zhang and Y. Hou, *Chem. Commun.*, 2008, 6576–6578.
15 S. D. Dalosto and Z. H. Levine, *J. Phys. Chem. C*, 2008, **112**, 8196–8199.
16 M. Han, B. Ozyilmaz, Y. Zhang, P. Jarillo-Herero and P. Kim, *Phys. Status Solidi B*, 2007, **244**, 4134–4137.
17 M. Y. Han, B. Ozyilmaz, Y. B. Zhang and P. Kim, *Phys. Rev. Lett.*, 2007, **98**, 206805.
18 X. L. Li, X. R. Wang, L. Zhang, S. W. Lee and H. J. Dai, *Science*, 2008, **319**, 1229–1232.
19 T. Ohta, A. Bostwick, T. Seyller, K. Horn and E. Rotenberg, *Science*, 2006, **313**, 951–954.
20 M. S. Toshiaki Enoki and M. Endo, *Graphite Intercalation Compounds and Applications*, Oxford University Press, 2003.
21 C. Casiraghi, S. Pisana, K. S. Novoselov, A. K. Geim and A. C. Ferrari, *Appl. Phys. Lett.*, 2007, **91**, 233108.
22 A. C. Ferrari, J. C. Meyer, V. Scardaci, C. Casiraghi, M. Lazzeri, F. Mauri, S. Piscanec, D. Jiang, K. S. Novoselov, S. Roth and A. K. Geim, *Phys. Rev. Lett.*, 2006, **97**, 187401.
23 A. C. Ferrari, *Solid State Commun.*, 2007, **143**, 47–57.
24 X. Xie, L. Ju, X. Feng, Y. Sun, R. Zhou, K. Liu, S. Fan, Q. Li and K. Jiang, *Nano Lett.*, 2009, **9**, 2565–2570.
25 H. C. Schniepp, K. N. Kudin, J.-L. Li, R. K. Prud,Äôhomme, R. Car, D. A. Saville and I. A. Aksay, *ACS Nano*, 2008, **2**, 2577–2584.
26 L. D. Landau, *Phys. Z. Sowjetunion*, 1937, **11**, 26–35.